

Power Control modeling and Simulation of Hybrid Power System for Building Microgrid Connected Application

Gi-Cap Yoon* · Jae-Hoon Cho · Won-Pyo Hong**

Abstract

In this paper, we propose to study the possibility of using a photovoltaic system combined with a high speed micro-turbine. This hybrid system can work as stand-alone system or grid connected system as it will be a part of a micro-grid. Initially, we propose Matlab/Simulink dynamic models of photovoltaic, micro turbine systems and supercapacitor. Then, we carry out a simulation comparison of the two systems, this is, with supercapacitor and without supercapacitor bank. We show that supercapacitor bank as short-term storage device was necessary to reduce the fast fluctuation of power in the case of sensitive loads. It is verified the simulation results of Matlab/Simulink based hybrid power system represent the effectiveness of the suggested hybrid power system.

Key Words : Matlab/simulink model, Hybrid power system, photovoltaic, gas microturbine, Supercapacitor bank, Microgrid

1. Introduction

A microgrid is a possible future energy system structure, which is based on small generation plants (photovoltaic, microturbine, fuel cells, etc.), together with storage devices (supercapacitors(SC), batteries and flywheels), and controllable loads [1-2]. Such systems can be interconnected to a low voltage distribution system or islanded mode operation. The advantage of the microgrid concept lies in a

significant reduction of CO₂ emissions for the following reasons [3]:

- The closed use of both electricity and heat increases the overall energy efficiency;
- Significant environmental benefits arise from the use of low or zero emission generators including PV arrays and fuel cells;
- Low impact on the electricity grid by a good match between generation and load, despite a potentially significant level of intermittent resemble energy based sources.

The production of photovoltaic system can vary slowly (day-night cycle and season change) and quickly because of weather conditions such as the passage of clouds. The power fluctuation might

* Main author : KEPRI of KEPCO
** Corresponding author : Hanbat National University
Tel : +82-42-821-1179, Fax : +82-42-821-1175
E-mail : wphong@hanbat.ac.kr
Date of submit : 2009. 11. 3
First assessment : 2009. 11. 4
Completion of assessment : 2009. 11. 11

cause problems of power quality. Moreover a grid connected photovoltaic system is considered as a negative load by the grid because of its uncontrollable characteristic. To reduce these problems, we can integrate a storage system which allows the energy management [4]. The hybrid power system is another interesting solution. It is using two or more renewable energy sources such as wind and/or solar it becomes more widely used [5]. The hybrid power system with, at least, one controllable source such as diesel generator or microturbine can solve this problem. This distributed generator is interesting because, it allow high efficiency with cogeneration system, low emission and fuel flexibility. This paper presents dynamic simulation study of a photovoltaic system and a microturbine operating within a multi-machine network[6]. Each generator can be connected via DC bus. Then, a single static converter is connecting this DC bus to the grid. In this work, we choose to connect it to the AC bus because the expansion of system is not limited by the rated power of the static

converter. Figure 1 shows the studied hybrid power system: a 17.3[kWp] photovoltaic system associated to a 28[kW] Capstone micro-turbine and 18[F]/480[V] Maxwell supercapacitors bank. It can operate as a stand-alone system or a grid connected system as it will be a part of a micro-grid.

2. Description and model of hybrid energy system

2.1 Microturbine generator(MTG)

2.1.1 Description of MTG

For this application, we have chosen a Capstone Micro Turbine Generator, Model C330, (MTG) [7]. The device is a recuperated single stage radial flow compressor and turbine on a single shaft integral with the generator. This MTG is composed of the following subassemblies: a Turbo Generator (TG); a two-way Frequency Converter AC-DC-AC (FC); a Fuel Control System (FCS); and a Digital Power Controller (DPC). The block diagram for the power source based on Capstone 28[kW] Micro-Turbine technology is represented in Figure 2. The Turbo Generator includes a Gas Compressor (GC), a Combustion Chamber (CC), a Turbine (T), a Heat-Recuperator (HR), and a High-speed Generator (PMSM). This model of Capstone MTG is equipped with a low NOx combustion engine and an internal natural gas compressor. These rotating components are mounted on a single shaft supported by air bearings. Air from the generator then flows into the GC where it is pressurized and forced into the cold side of the HR. Exhaust heat is used to preheat the air before it enters the Combustion Chamber and thus reduce fuel consumption by about 50 percent. Then, the CC mixes the heated air with fuel and burns it. This mixture expands

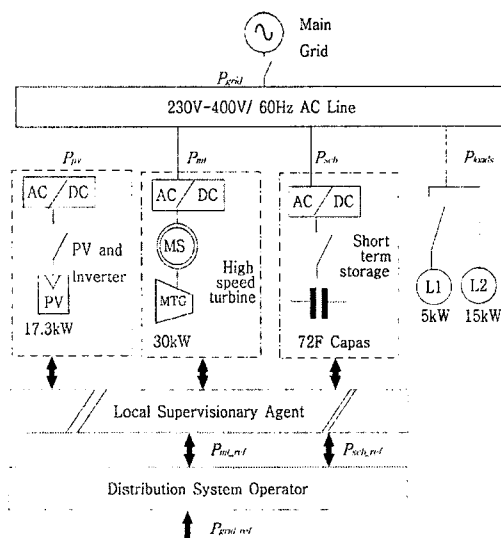


Fig. 1. PV/MTG/Supercapacitor micro-grid control scheme

through the turbine, which drives the GC and generator at up to 96,000[RPM]. The combusted air is then exhausted through the heat recuperator before being discharged at the exhaust outlet. The used High-speed Generator is a two-pole Permanent Magnet Synchronous Machine (PMSM) with a non-salient rotor. This PMSM generator is cooled by the air flow into the Micro-turbine, and the output of the generator is a variable-voltage system, variable-frequency AC power at up to 1,600[Hz]. At 1,600 Hertz (96,000 [RPM]), the machine output power is 28[kW] and

its terminal line-to-line voltage is 400[V]. Two back-to-back power converters are used to generate 50 or 60[Hz] quantities to the grid. Generally, a one way frequency converter AC-DC-AC with a diode rectifier is used to interface the high frequency alternator and the DC bus [8]. The Capstone C330 model uses a two-way frequency converter AC-DC-AC: the power structures of both electronic converters are identical [8]. It can be shown that for this model of MTG, the generated current harmonics are adequately attenuated by the machine inductance and by the grid LC-filter [8].

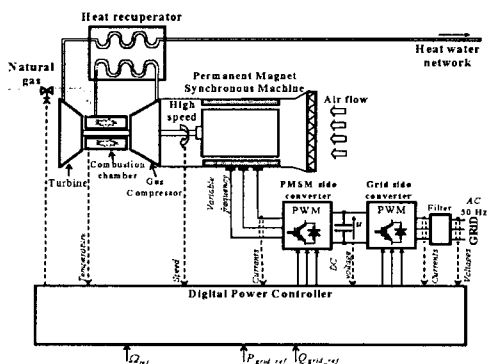


Fig. 2. Microturbine control scheme

Table 1. PMSG Parameters

Permanent magnet synchronous machine(PMSM)	480[V], I=36[A], f=1,600[Hz]
Number of poles	$P=2$
Direct and quadrature inductances	$L_d=L_q=6.875 \times 10^{-4}$
Stator resistance	$R_s=0.25[\Omega]$
Flux induced by the permanent magnet	$\Phi_m=0.0534[\text{wb}]$
DC bus capacitor	$C= 5,000[\mu\text{F}]$
PI controller sampling period	100[μs]
Speed governor parameters (isochronous governor)	Gain (K) = 25, X=0.4, Y=0.05, Z=0
Load parameters	25[kW], 480[V], 60[Hz]

2.1.2 MTG model

The simplified single shaft gas turbine including its control systems which is implemented in Simulink of the Matlab is represented in reference[8]. The model consists of fuel control, turbine dynamics and speed governor blocks. The electromechanical behavior is of main interest in this work. The speed control operates on the speed error formed between a reference (one per-unit) speed and MTG system rotor speed. It is the primary means of control for the MT under part load conditions [9]. To remove such limitations in the dynamics of the power sources some form of storage system is necessary at the AC or DC bus to cope with instantaneous changes in power demand. In an island mode, this is critical in the case of sensitive loads, because micro-grids will be incapable of meeting load requirements if a storage system is not included [10].

2.2 Photovoltaic system model

2.2.1 Description of the PV system

The photovoltaic studied system, presented in figure 2, consists of 108 160[Wp] BP Solar modules. These modules are connected to a

3-phased grid via six inverters IG30 (one inverter connects 2 branches of 8 modules in parallel). In the first year of electric production, this 17.3[kWp] PV-system generated 13,600[kWh] as shown in figure 3.

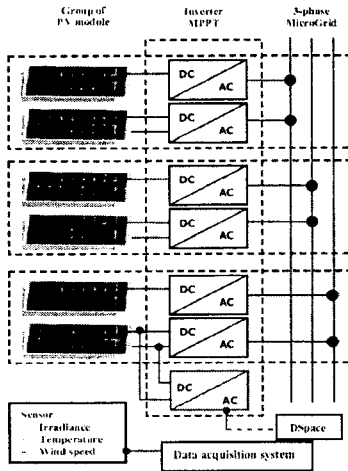


Fig. 3. Photovoltaic control scheme

2.2.2 PV modelling and simulation

The traditional equivalent circuit of a solar cell represented by a current source in parallel with one diode is shown in figure 4. This single-diode model [11] includes four components:

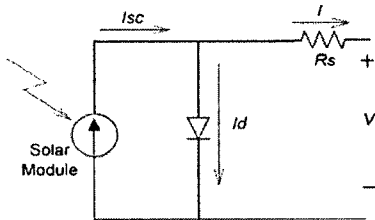


Fig. 4. The solar cell equivalent : single diode model

a photo current source I_{ph} , a diode parallel to the source (V_D, I_D), a series resistor R_s and a shunt resistor R_{sh} . In most cases, it is difficult to obtain these five parameters mathematically, due to the

exponential equation of the p-n diode junction. In a previous work, W. Xiao and als. compared two photovoltaic modules models: the classical one-diode model and a simplified one-diode model where the shunt resistor R_{sh} was neglected [12]. This model requires four parameters derived from data that can be obtained from commercial PV-modules under three conditions: short circuit current I_{sc} , open circuit voltage V_{oc} , and the I - V characteristics for different temperature levels at constant solar irradiance ($1,000[W/m^2]$) as shown in figure 5. Fig. 2 shows the equivalent circuit model of a PV module. This circuit model is composed of an ideal current source, a diode connected in parallel with the current source and a series resistor. As a function of voltage, the output terminal current I may be described by the implicit Eq. (1) in Fig. 2.

$$I = I_{sc} - I_0 \left(\exp\left[\frac{V + IR_s}{nV_T}\right] - 1 \right) \tag{1}$$

where, I_0 is the diode saturation current [A]; V is the terminal voltage of a module [V]; n is the ideal constant of diode; V_T is the thermal potential of a module [V], V_T is the $m(kT/q)$; k is the Boltzmann's constant ($1.38e^{23}$ [J/K]); T is the cell temperature [K]; q is the coulomb constant ($1.6e^{19}$ [C]); m is the number of cells in series in a module. The short circuit current I_{sc} depends on solar irradiance S and cell temperature T and can be represented by (2).

$$I_{ph} = I_{sc} = I_{sc0} \left(\frac{S}{S_{us}} \right) + J(T - T_s) \tag{2}$$

Applying the open circuit, open circuit voltage is expressed by (3)

$$V_{oc} = V_{oc0} + \Delta V_{oc}(T - T_s) \tag{3}$$

Where, T_s is the reference cell temperature (298[K]); I_{sc} is the short circuit current[A]; S is the irradiance[W/m²]; J is the temperature coefficient at short circuit current[A/K]; S_{as} is the reference irradiance, 1,000[W/m²]. The open circuit condition (i.e. $I = 0$ and $V = V_{oc}$ in Fig. 4), The diode saturation current $I_{0,ref}$ at T_s can be obtained as below:

The diode saturation current I_0 varies with temperature and can be expressed as (4).

$$I_0 = I_{sc} \frac{1}{\exp\left[\frac{V_{oc}}{nV_T}\right] - 1} \approx I_{sc} \cdot \exp\left[-\frac{V_{oc}}{nV_T}\right] \quad (4)$$

$$I_0 = AT\gamma e^{\left(-\frac{E_g}{nKT}\right)}$$

Where, V_{oc} is the open-circuit voltage [V]; V_{ocs} is the open-circuit voltage at S_{as} and T_s [V]; ΔV_{oc} is the temperature coefficient of open-circuit voltage; A is the temperature coefficient of

saturation current; T is the temperature dependency coefficient [3]; E_g is the band energy gap[eV]; $1eV=1.6 e^{-19}$ [J]; n is the ideal constant[1,5].

A PV array consists of a group of modules that are connected in series-parallel combinations. Based on Eq. (1) and the circuit of Fig. 4, Output current I_A of a PV array with NS modules in series and NP in parallel may be represented by (5).

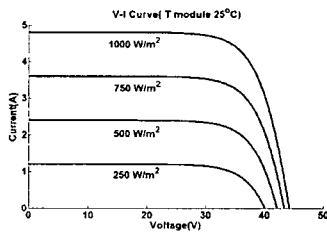
$$I_A = N_p I_{sc} - N_p I_0 \left(\exp\left[\frac{V_A + I_A R_s}{n N_s V_T}\right] - 1 \right) \quad (5)$$

Figure 5 show the simulated $I-V$ characteristics of the studied BP solar 3,160 modules.

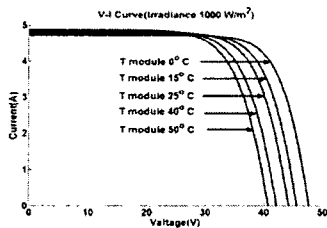
2.3 Supercapacitor bank(SCB) system model

A SCB is useful for the compensation of fluctuation powers since it is capable of controlling both real and reactive powers for the benefit of power quality. It handles an Electric Double Layer Capacitor (EDLC) module with power electronic converters. The 144[F]/48[V] EDLC is a self-constrained energy storage device, storing up to 161[kJ] (44.8[Wh]) of energy. It includes eighteen individual super capacitor cells, bus bar connections, and an integral active cell balancing circuitry[13]. Two modules are connected in series to obtain higher operating voltage and storage energy for our microgrid application. The module characteristics are shown in Table 2.

The SCB is composed of the Super Capacitor (SC), a SC filter, a chopper, a DC bus, an inverter and a three-phase grid filter (Fig. 2). The first step of the SCB multi-level modeling is consists to gather dynamical equations of each element into 'ProX' and 'ES'macro blocs in order to obtain an EMR.



(a) the characteristics for different irradiance level and constant temperature (25(°C))



(b) the characteristics for different temperature levels at constant solar irradiance(1,000(W/m²)s

Fig. 5. I-V characteristics of a BP solar 3160 PV module

Table 2. Parameters of the used ELDC

Parameters	Value
Capacitance(C_0)	144[F] + 20[%] initial
Voltage	48.6 Volts DC Max.
DC Resistance (R_s)	11[MΩ] Max., initial
Capacitor Cycle	1,000,000
Operating temperature range	-40[°C] to +65[°C]

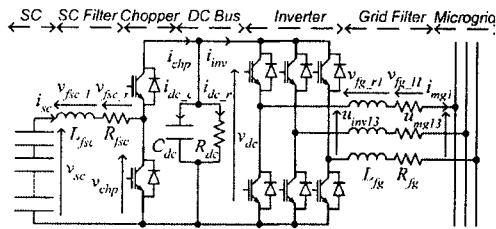


Fig. 6. Electric scheme of the SCB

2.3.1 Modeling of the SC

The super capacitor module is modeled as a voltage source. For the study of power system applications, the model of Zubieta and Bonert [14] can be applied. Nevertheless, for the simplification of the study, the model with a resistor R_s and a ideal capacitor C_0 in series is used.

$$\frac{dv_c}{dt} = \frac{1}{C_0} i_{sc} \tag{6}$$

$$v_R = R_s i_{sc} \tag{7}$$

$$v_{sc} = v_c + v_R \tag{8}$$

2.3.2 Modeling of the filter

The SC filter is modeled as an inductance (L_{fsc}) and a resistance (R_{fsc}) in series.

$$\frac{di_{fsc}}{dt} = \frac{1}{L_{fsc}} v_{fsc-l} \tag{9}$$

$$v_{fsc-l} = v_{sc} - v_{chp} - v_{fsc-r} \tag{10}$$

$$v_{fsc-r} = R_{fsc} i_{sc} \tag{11}$$

2.3.3 Modeling of the chopper

The chopper adapts the low voltage across the supercapacitor to the desired voltage for the DC bus. An equivalent continuous model [8] of the chopper is used by a mean value modulation function m_{chp} :

$$v_{chp} = m_{chp} v_{dc}$$

$$i_{chp} = m_{chp} i_{sc}, \quad m_{chp} \in [0,1] \tag{12}$$

2.3.4 Modeling of the grid-side DC bus

The DC bus is considered as a capacitor (C_{dc}) and a resistance (R_{dc}) in parallel.

$$\frac{dv_{dc}}{dt} = C_{dc} i_{dc-c} \tag{13}$$

$$i_{dc-c} = i_{chp} - i_{inv} - i_{dc-r} \tag{14}$$

$$i_{dc-r} = \frac{1}{R_{dc}} v_{dc} \tag{15}$$

2.3.5 Modeling of the inverter

Equivalent mean modeling of the power converters [8] is sufficient for the study. It represents fundamental phase-to-phase voltage $u_{inv} = [u_{inv13}, u_{inv23}]^T$ and line currents $i_{mg} = [i_{mg1}, i_{mg2}]^T$ components as:

2.3.6 Modeling of the three-phase filter

The line current i_{mg} are deduced from the inverter voltages u_{inv} and the grid voltages $u_{mg} = [u_{mg13}, u_{mg23}]^T$.

$$\frac{d}{dt} i_{mg} = \frac{1}{L_{fg-l}} \tag{16}$$

$$v_{fg-l} = \frac{1}{3} \begin{bmatrix} 2 & -1 \\ -1 & 2 \end{bmatrix} (u_{inv} - u_{mg}) - v_{fg-r} \tag{17}$$

$$v_{fg,r} = R_{fg} i_{mg} \tag{18}$$

where L_{fg} and R_{fg} are the inductance and resistance of the filter, the $v_{fg,l} = [v_{fg,l1}, v_{fg,l2}]^T$ and $v_{fg,r} = [v_{fg,r1}, v_{fg,r2}]^T$ are the voltages respectively across L_{fg} and R_{fg} .

2.3.7 Modeling of the microgrid

The grid voltages u_{mg} is modeled by :

$$u_{mg} = \begin{bmatrix} u_{mg13} \\ u_{mg23} \end{bmatrix} = \sqrt{2} A \begin{bmatrix} \sin(2\pi ft - \frac{\pi}{6} + \theta_0) \\ \sin(2\pi ft - \frac{\pi}{2} + \theta_0) \end{bmatrix} \tag{19}$$

where A is the rms value of the grid phase-to-phase voltage, f is the grid frequency and θ_0 is the initial angle of the grid voltage. The line currents i_{mg} are considered as disturbances for the microgrid.

Fig. 7 shows the Matlab/Simulink SCB component model developed in this study. This model is composed of SCB, bidirectional DC-DC converter, converter and LCL filter connected to the grid. This model is validated by simulation in [10].

3. Configuration of hybrid power system

The global system has three control inputs in order to manage the system. The inverter has two independent modulation functions m_{inv1} and m_{inv2} using its switching orders. The chopper has only one modulation function m_{chp} . The control task is to reduce the power variations of the microgrid. The inverter is used to control the real and reactive power at the connection point. The control input of the chopper is used to control DC bus voltage, since the voltage of the DC bus must be constant for correct system performances. The control system is ordered by the following

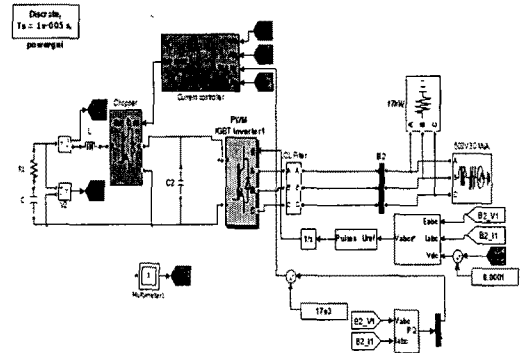


Fig. 7. Malta/Simulink SCB model

steps according to the rules of the multilevel representation.

The SC terminal voltage v_{sc} changes very slowly thanks to a great quantity of stored energy. The DC bus voltage v_{dc} has also a slow dynamic, since it has to be controlled as constant in order to ensure the inverter function. At the ac side, the principal component of all quantities (voltages and currents) is 50 or 60[Hz]. By modeling them into a 50[Hz] rotational Park form, they become stationary. Moreover if their magnitudes are constant, they can be considered constant as u_{mg} for the microgrid voltages. Figure 8 shows the converters and control system block diagram. This hybrid power system is composed of two

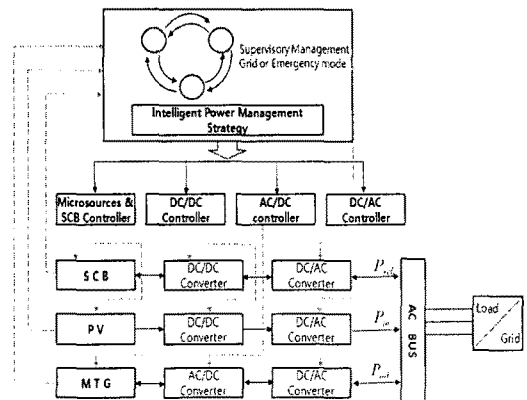


Fig. 8. Converter control configuration for hybrid power system

microsources and one electric storage of SCB. Each microsources have the various converters to control the power in a AC bus.

The accurate and robust controllers are needed to reduce the power fluctuation in AC bus. DC/DC, AC/DC and DC/AC controllers are implemented by Matlab/Simulink tool. In order to manage the power of hybrid power system(HPS) effectively, The decision of operation and their controller for HPS, the active power setting of DE units and load control are carried out by the intelligent power management strategy. Especially, for security reasons, it should be between the maximal allowed value and 50[%] of this value for an efficiency reason. If this voltage is under 48[V], the SCB can not operate in a generation mode.

4. Simulation results

4.1 Microgrid power management

The modeling and the control system of the micro turbine and the photovoltaic plant are designed by the same method[10]. The coupling of these three systems is performed by the sum of currents at the connection point to the microgrid. The modeling of the power flow for the microgrid in generation mode can be described by the Fig. 9.

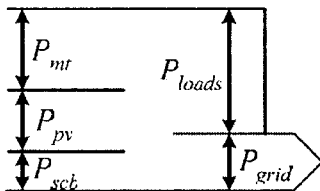


Fig. 9. Power flow for the microgrid in generation mode

The microgrid real power exchanged with the grid P_{grid} is the sum of the micro turbine generation system P_{mt} , the photovoltaic generation

system P_{pv} , the SCB P_{scb} and loads P_{loads} (Fig. 1).

$$P_{grid}(t) = P_{mt}(t) + P_{pv}(t) + P_{scb}(t) - P_{load}(t) \quad (20)$$

4.2 Description of the PV–Micro turbine hybrid system

The association of a photovoltaic system and a microturbine allows the power management:

- In a stand-alone system, the difference between the photovoltaic energy and loads is adjusted by the micro turbine which means energy storage system is not necessary.
- In a grid-connected system, in which the energy is controllable, this system can be considered by the grid as a small power plant, not only as a negative load. To analyze to power characteristics of hybrid energy system(HES), the fully detailed Matlab/Simulink model of HES was implemented. Figunot a shows the full Matlab/Simulink model of HES connected to as impNonlinear power converter and their controller to operate HES was also implemented. The

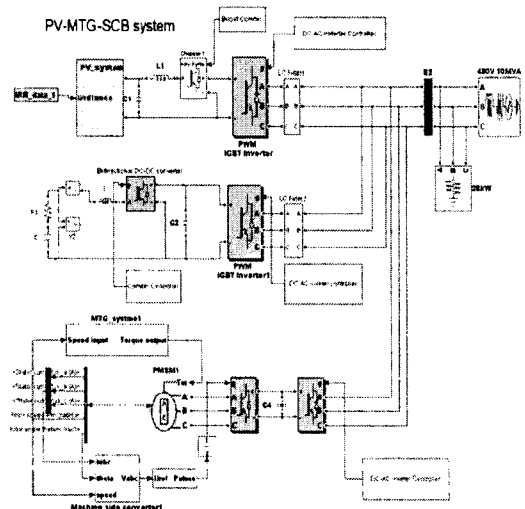


Fig. 10. Matlab/Simulink model of HES

power condition system include a AC-DC and DC-AC converter for microturbine, DC-DC and DC-AC converter for photovoltaic and buck-boost DC-DC and DC-AC converter for supercapacitor.

4.3 Simulation of the PV-Micro turbine hybrid system

Simulations depicted in Figure 11 show the case with only active power exchange with the utility grid. The solar radiation varies in steps every 0.2s in the way described in the figure, producing changes in the maximum power drawn from the PV array. As can be observed, the P&O method proves to be accurate in following the MPP of the solar system, for an optimum duty cycle perturbation step in accordance with the chopper dynamics.

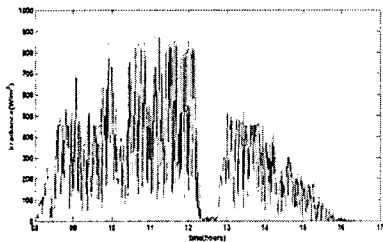


Fig. 11. Photovoltaic power

Figure 12 shows the various powers with an applied reference electric power of 28[kW]. The simulated results prove the effectiveness of the proposed solution. We can notice that the MTG practically compensate all the PV fluctuations of power. Nevertheless, to reduce the fast fluctuations of power, we propose to use a 14[F]-400[V] 23[kW] supercapacitors bank [13].

Figure 13 shows the various powers with an applied reference electric power of 28[kW].

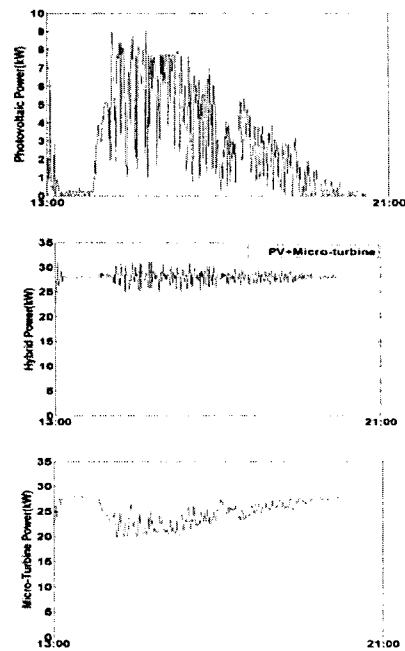


Fig. 12. Power of PV/MTG Micro-grid

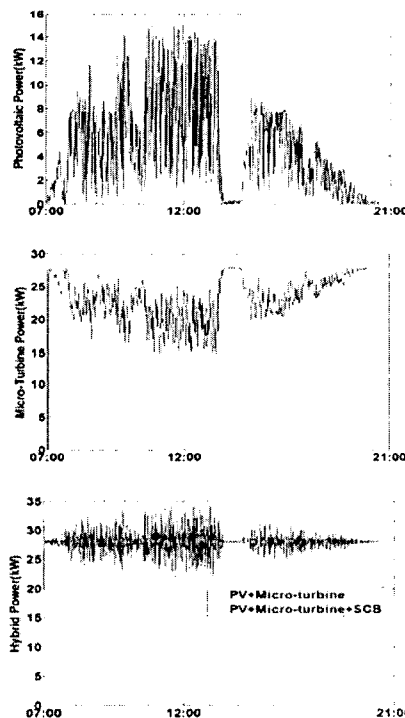


Fig. 13. Power of PV/MTG/SCB micro-grid

5. Conclusion

Initially, we carried out a detailed and effective Matlab/Simulink modelling of the PV, MTG generators and supercapacitor, their power conditioning system and their controller to operate HES. Lastly, we showed that short-term storage was necessary to reduce the fast fluctuations of power in the case of sensitive loads. We can observe the fast power fluctuations due to the slow response time of the micro turbine are reduced by the short term energy storage system SCB. The SC terminal voltage is well controlled between 48[V] and 96[V]. We propose to use supercapacitors to reduce them.

Acknowledgment

The authors would like to gratefully acknowledge the financial support of KESRI (Korea Electrical Engineering & Science Research Institute) under project R-2007-1-015-02

References

- [1] Abu-Sharkh A. et al. "can microgrid make a major contribution to UK energy supply?," *Renewable and Sustainable Energy Reviews* 10, pp.78-127, 2006.
- [2] W. Lasseter, et al., "Integration of Distributed Energy Resources - The Microgrid Concep" *CERTS Microgrid Review*, 2002. Feb.
- [3] R. Lasseter, "Dynamic models for micro-turbines and fuel cells" 2001 IEEE Power Engineering Society Summer Meeting, pp. 761-766 vol.2. 2001.
- [4] W.P.Hong, "Control and operation of building Microgrid," *KIEE Magazine*, Vol.23, No. 2, pp.10-23, 2009.
- [5] W.P.Hong, "Modeling, Control and Simulation of Microturbine Generator for Distributed Generation System in Smart Grid Application," *KIEE English Journal*,
- [6] S. F. Gillette, "QHP Case Studies - Saving Money and Increasing Security", Capstone Turbine Corporation.
- [7] <http://www.capstoneturbine.com>
- [8] R.J. Yinger, "Behavior of Capstone and Honeywell Microturbine Generators During Load Changes" *CERTS Report LBNL-49095*, July 2001.
- [9] R.J. Yinger, "Behavior of Capstone and Honeywell Microturbine Generators During Load Changes" *CERTS Report LBNL-49095*, July 2001.
- [10] O.Fethi, L.-A. Dessaint, K. Al-Haddad, "Modeling and

simulation of the electric part of a grid connected microturbine", 2004 IEEE Power Engineering Society General Meeting, Vol.2, pp. 2212-2219, 2004. 6-10 June.

- [11] L. N. Hannett, A. Khan, "Combustion turbine dynamic model validation from tests" *IEEE Trans. On Power Systems*, Vol. 8, No. 1, 1993.
- [12] W. Xiao, W.G. Dunford, A. Capel, "A novel modeling method for photovoltaic cells", *IEEE Power Electronics Specialists Conference*, Aachen, Allemagne, 2004.
- [13] Maxwell technologies application note, "How to determine the appropriate Size Ultracapacitor for your application", document 1007236 Rev 2, October, 2004.
- [14] L. Zubieta, and R. Bonert, Characterization of double-layer capacitors for power electronics applications, *IEEE Trans. Ind. Appl.*, Vol. 36, No. 1, pp. 199-205, 2000.

Biography

Gi-Cap Yoon

Gi-Cap Yoon received the B.S., M.S, and Ph. D. degrees in Electrical Engineering from Hanyang University, Seoul, Korea, in 1983, 1988, and 1999. He is presently a senior researcher in distribution power system lab. and advanced distribution system group at KEPRI. His research field includes wind power generation system, distribution generation system, and control of power system.

Jae-Hoon Cho

Jae-Hoon Cho received the M.S degree in Control & Instrumentation Engineering from Hanbat National University in 2002, Korea. He is working toward the Ph.D. degree in the Electrical & Computer Engineering at Chungbuk National University, Korea. His interests are evolutionary computation, swarm intelligence, pattern recognition, neural network, bioinformatics.

Won-Pyo Hong

Won-Pyo Hong was born in Daejeon city in the Republic of Korea, on May 15, 1956. He received the B.S. degree from the electrical engineering from the Sungsil University, Seoul Korea, in 1978 and M.Sc. and Ph.D. degrees in electrical engineering from Seoul National University, Seoul, Korea, in 1980 and 1989, respectively. From 1980 to 1993, he was senior researcher of the Korea Electric Power Research Institute at the Korea Electric Power Cooperation. he was visiting professor at the UBC, Canada, from 2007 to 2008. He is a professor at the department of Building Services Engineering of Hanbat National University, where he has taught since 1993. His main research interests are building energy and management system, green buildings, fieldbus based control and distributed energy resources.